Influence of several relaxation times on the cryogenic self-heating of silicon devices

F. Javier De la Hidalga-W and Mauro Landa-V
Departamento de Electrónica
Instituto Nacional de Astrofísica, Óptica y Electrónica, INAOE.
P.O. Box 51 y 216, Z.P. 72000, Puebla, Mexico

The first experimental determination of self-heating in silicon devices operating at low temperatures was based on their transient response; there have been, however, some concerns regarding the validity of this approach. In this work, we compare several electrical relaxation times with the temperature dependent thermal time constant of a silicon sample for the 5K<T<300K temperature range. The electrical relaxation times were calculated for the most common processes that are responsible for the relaxation of the depletion region at low temperatures. We found that thermal transients are undistinguishable from the electrical transients for low/moderate electric fields and nondegenerate uncompensated silicon samples operating at liquid helium temperatures. These results disagree with the assumption widely used at room temperature, which establishes that thermal events are much slower than the relaxation of the depletion region.

Keywords: Low Temperature Electronics, Silicon devices, Cryogenics, Self-Heating, Depletion Region, Relaxation, Thermal Transient, MOSFET

1. Introduction

Si-based read-out electronics has been used to amplify and/or to multiplex electrical signals delivered by radiation detectors operating at very low temperatures (LT) [1,2]. In order to avoid the undesirable deterioration of the signal-to-noise ratio, speed of response and heat leakages, the Si circuitry has to be as close as possible to the cryogenic detectors, thus operating at similar temperatures. Si devices can, however, show important degradation in performance when operated under deep cryogenic conditions [1]. Several detrimental effects such as kink, hysteresis, excessive noise, and drain threshold voltage have been thoroughly studied for cryogenic Si-JFETs and MOSFETs [1,3]. On the other hand, non-electrical effects such as self-heating (SH), have rarely been studied for Si devices operating at temperatures below 300 K.

Under deep cryogenic conditions, the behavior of the thermal properties of most solids differs qualitatively and quantitatively from that at room temperature (RT) [4]. The variation of thermal conductivity, κ_{th}, with temperature in Si is shown in Fig.1. This was obtained with the phenomenological model of Callaway [5,6], and the phonon relaxation times were calculated using the parameter values from Glassbrenner and Slack [7]. In this figure, the specific heat of Si, C_{Si}, is also included; this was calculated using the well-known Debye's model [8].

Since the thermal conductivity and the specific heat decrease significantly with the lowering of the temperature, it is believed that the SH becomes stronger under such conditions. It is also known that under deep cryogenic conditions, several semiconductor parameters such as charge carrier concentration, intrinsic concentration, mobility, diffusivity, generation/recombination lifetime, as well as the transport mechanisms depend strongly on the operating temperature [9]. Hence, The study of the cryogenic SH of semiconductor devices becomes a fundamental issue since the localized variations of the device's temperature can significantly alter their operating conditions at LT

In spite of the several experimental findings regarding the cryogenic SH of Si devices [10-15], little effort, if any, has been expended in order to understand the actual origin of the measured temperature rise and the observed transients. The transient response to a voltage step was used as a monitor for SH [11-13], regardless of the appropriateness of the assumptions on which this technique is based: thermal transients were assumed to be the slowest processes during the relaxation of the sample; thus the slow variation of the current was ascribed to the heating of the device.

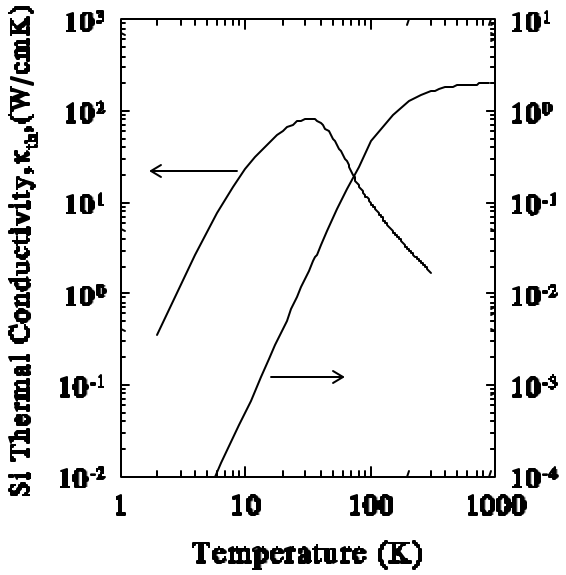

Figure 1. Thermal conductivity and specific heat of silicon as a function of temperature.

However, and according to Fig. 1, the thermal time constant must decrease exponentially at very low temperatures due to its direct dependence on C_{Si}, whereas the relaxation of the depletion region must occur at a slower rate because of the freezing-out of carriers in the quasi-neutral region of the sample. The aim of this work is to investigate the appropriateness of the transient response method to measure the SH as well as the region of dominance of several processes leading to such transient. To achieve this goal we estimate several electrical relaxation times; these times are thus compared to the theoretical thermal time constant of a Si sample in the 5K<T<300 K range. In Sec. II we present a brief review of earlier experimental data regarding the SH of Si devices and several anomalies are pointed out; they lead to the conclusion that those results were misinterpreted. Some mechanisms responsible for the slow relaxation of the depletion region are presented in Sec. III, and simple estimations of several relaxation times are compared and discussed in Sec. IV.

2. Cryogenic self-heating of silicon devices

Since the first experimental studies on silicon MOSFETs, Sesnic and Craig [11] suspected that the effective temperature of the active part of the device was much higher than the 4.2 K ambient temperature. The main reason for such conclusion was the fact that some electrical parameters changed very little when the temperature was lowered from 77 K to 4.2 K, while a substantial change was observed when the temperature was lowered from 300 K to 77 K. In [11], the authors use the temperature variation of the transconductance as the self-heating monitor.

The saturation observed for T<77 K is indeed affected by the device's self-heating. However, such saturation is also the combined result of the weak temperature dependence of several parameters which may present a much stronger temperature dependence for T>77 K. For instance, mobility may saturate as a result of neutral impurity scattering (in the case of a heavily doped uncompensated substrate) [1]. The threshold voltage, which also determines the transconductance, usually presents a saturation-like behavior at temperatures below 77 K [16]. This effect is linked to the weak temperature dependence of the band-gap and the potential barrier through the depletion region.

Although their observations are unclear, their conclusions are not too far from posterior experimental results. Other authors measured comparable temperature rises [11-13]; some of these results are shown in Table 1 for self-heating in MOSFETs. In [11], Sesnic and Craig applied a steep risetime voltage step on the drain of an n-MOSFET, and the temporal change of the drain current was recorded. It was assumed that this change reflected the transient increase of the temperature of the channel.

Table 1. Results of self-heating in MOSFETs operating at low temperatures; these were measured by using the *transient drain current* method.

Measured Time Constant	Device Area (mm^2)	Power (mW)	T_{amb} (K)	DT (K)	[Ref]
τ_{th}=1 µs @ 4K<T<40K τ_{th}=10 ms @ 40K<T<45K	---	15	4.2	40	[11]
τ_{th}>60 s	760	30	20 80 200	24 10 9	[12]
τ_{th}>60 s	3143	46-60	20 80 200	24 12 11	[13]

It was implicit that the thermal time constant (τ_{th}) of this device at such temperatures was much longer than any electrical relaxation time. So that, the initial drain current, $I_{DS}(t=0)$, was taken as its value at the ambient temperature, $I_{DS}(T=T_{amb})$, as the self-heating process had not started yet increasing the device temperature. By taking this initial value for different ambient temperatures, a calibration curve $I_{DS}(t=0)$- T_{amb} was obtained. The value of I_{DS} for a later time was taken as the value of I_{DS} corresponding to the local temperature $T=T_{amb}+\Delta T$, ΔT being dependent on time. The steady state value of I_{DS} was recorded after the transient, and the equivalent temperature is the value shown in the first row of Table 1, and two different values for the thermal time constant were observed for two ranges of temperature.

A similar *transient drain current* (TDC) approach was used by Foty and Titcomb for an n-MOSFET [12], and

by Foty for a p-MOSFET [13]. In both of these works, the authors characterized ΔT for different power levels and for the wide temperature range of 20 K<T<200 K. A thermal time constant of the order of minutes was obtained regardless of the type of device, the ambient temperature and the power level. This τ_{th} is five orders of magnitude longer than the value measured by Sesnic and Craig. Besides this extremely long τ_{th}, another anomaly is observed in their reported ΔT. By comparing the second row (n-MOSFET) with the third row (p-MOSFET) of Table 1, one can observe that a very similar ΔT was obtained under similar conditions, despite the difference on device areas. The p-MOSFET area is 4-times the area of the n-MOSFET. Hence, and for a first hand estimation, a higher ΔT should have been expected for the smaller device, as its geometry dependent thermal resistance, R_{th}, should have been higher.

Regardless of the anomalies already mentioned, the TDC approach is based on a wrong assumption. Such heating transient (if the heating were the responsible for the transient) must represent how long the heat generated in the channel takes to reach the heat sink (the bottom part of the substrate or the chip package), and not the heating of the channel. Actually, the device temperature must increase sharply (because of the very low value of C_{Si}) to a maximum value just after the voltage is pulsed, and then must start decreasing to the steady state value as the heat is being transferred. In other words, the transient observed in [11-13] seems to be not the result of the heating but of the cooling of the channel (T going from the initial peak value to the steady state value). Hence, what the authors took as $I_{DS}(T=T_{amb})$ was actually the value of $I_{DS}(T=T_{max})$.

Although the use of the TDC technique to quantify ΔT is questionable, it gave some insight on the value of the time constants involved at low temperatures. These transients, however, may not be due to thermal phenomena. According to the results presented in Table 1, the values of those time constants show a large dispersion. Sesnic and Craig [11] observed a strong temperature dependent time constant: 1 μs for 4.2 K<T<40 K and 10 ms for 40 K<T<45 K. On the other hand, Foty [12,13] reported a temperature independent (for 20 K<T<200 K) time constant of the order of minutes. As a support for the former results, one can mention the time constant reported by Gutiérrez et al. [14], whose values and temperature dependence are similar to those obtained in [11]: 1 μs at 20 K, 5 ms at 33 K and longer than 50 ms at 37 K. Gutiérrez-D et al. [14] measured ΔT in a resistor by using another diffused resistor as a thermometer; these resistors were diffused in the Si substrate very close to each other. Thermal transients were recorded as a response to voltage steps with very steep edges. The thermal nature of these time constants can be verified by comparing them with the expected $\tau_{th.}$. An analytic calculation of τ_{th} is not possible; a solution of the non-linear 3-D heat conduction equation must be found. However, an approximate 1-D solution can be used to visualize both the order of magnitude and the temperature dependence of τ_{th}. This can be done by taking the simple model of the thermal network for the silicon device shown in Fig. 2.

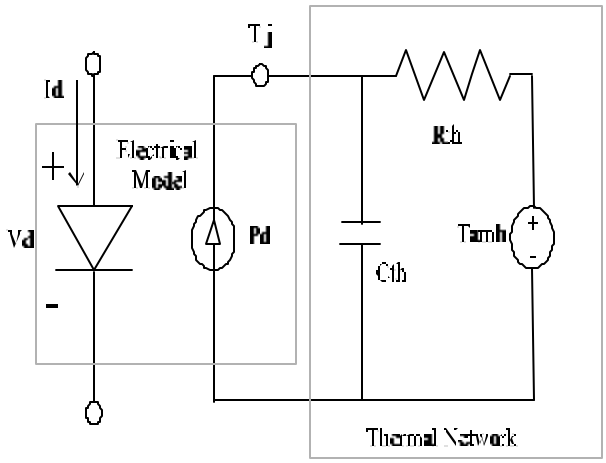

Figure 2. Electro-thermal model of a diode [17]. The electrical parameters of the diode depend on $T_j=DT+T_{amb}$.

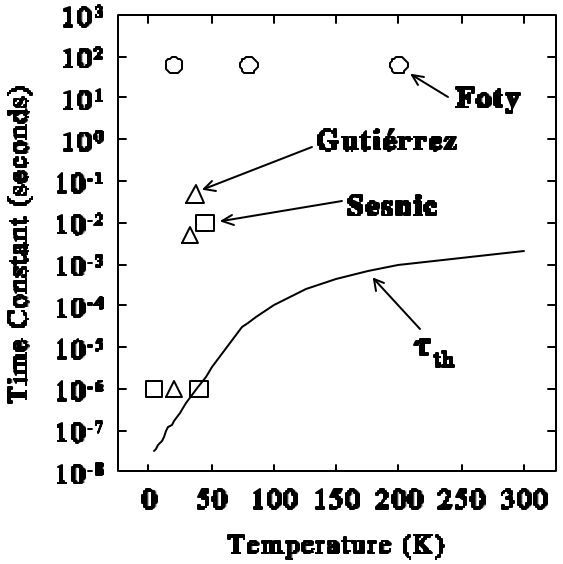

Figure 3. Calculated thermal time constant as a function of temperature for a typical silicon substrate. Some experimental data [11-14] are included for comparison.

The *circuital* thermal time constant will simply be:

$$\tau_{th} = R_{th} C_{th} \qquad (1)$$

The thermal capacitance C_{th} is given by $(a^2\ell)\, C_{Si}$. The cross section and the length of the sample are a^2 and ℓ, respectively. The thermal resistance is given by $\ell/(a^2 K_{th})$. Hence, (1) can be written as:

$$t_{th} = \frac{\ell^2 C_{Si}}{K_{th}} \qquad (2)$$

The thermal time constant expressed by (2) is plotted in Fig. 3 against temperature. The values of K_{th} were taken from Fig. 1 and a typical substrate thickness of 500

μm was assumed for ℓ. It can be seen that the value of τ_{th} may range from 32 ns at 4.2 K up to 2 ms at room temperature. This represents a variation of five orders of magnitude in this temperature range.

As can be seen in Fig. 3, the time constants measured by Foty [12,13] behaves very different to the theoretical $\tau_{th.}$ Although a quantitative comparison is not possible in principle, it can be seen that the τ_{th} measured by Sesnic and Craig [11] and Gutiérrez [14] are not too far from the theoretical estimation. Nevertheless, they reported a much stronger variation for temperatures around 40 K. This may be due to occurrence of slower relaxation processes, such as the formation of the depletion region.

3. Forced depletion region formation

The behavior of the RT depletion region is well-known; if a reverse bias is applied to a p-n junction, to a Schottky diode, or to the gate of an MOS device, the free carriers are instantaneously swept away by the surface electric field, resulting in the widening of the space charge region. This depletion region is always in thermal equilibrium and the time constant to reach it is dominated by the dielectric redistribution of free carriers. This relaxation has a very short time constant, inversely proportional to carrier concentration, much shorter than microseconds for any reasonably free carrier concentration.

At intermediate temperatures (30 K< T < 200 K), with no hard freeze-out, the time constants are limited by thermal emission and recombination, processes that are absent in deep cryogenic conditions.

At very low temperatures, shallow impurities in silicon devices are largely frozen-out in a neutral charge state. After applying a reverse bias, the trapped carriers are emitted from the impurities and swept out by the electric field until the depletion region returns to equilibrium, i.e. fully ionized. The long time constant involved in this process may be governed by shallow level impact ionization and recombination of impurities in MOSFETs [1] or by Poole-Frenkel mechanism in pn-junctions [23,24]. Some experimental evidence of this transient and field-dependent depletion region formation have been reported since the work of Saks et al. [19]. Rosencher et al. [24] have successfully modeled and simulated the Poole-Frenkel mechanism dependent transient current in silicon p-n junctions.

Below 30 K, there are virtually no free electrons or holes present at equilibrium in neutral, zero electric field, nondegenerate silicon. At deep cryogenic temperatures, thermal ionization is absent, and only under non-equilibrium conditions dopants can be ionized. Return to equilibrium occurs with the trapping lifetimes for shallow ionization, which become shorter as the temperature drops. The possible mechanisms of emission from shallow level at low temperatures, as well as the respective emission rates are the following:

-Thermal ionization; it is the dominant mechanism at high temperature, and the emission rate is given by [1]

$$e_0(T) = A_0 T^2 \exp\left(\frac{-E_i}{K_B T}\right) \qquad (3)$$

where A_0 is a constant ($3.33\text{x}10^8$ s^{-1}), K_B is the Boltzmann's constant, E_i is the activation energy of the trap and a T^{-2} dependence is assumed for the trap cross section [18].

-Field assisted thermal emission (Poole-Frenkel); represents an enhancement of the thermal emission given by (3); this is due to the lowering of the electrostatic barrier of the impurity ion by an electric field [19,20]

$$A_{PF}(T,\vec{F}) = A_0 T^2 \exp\left(\frac{-\left(E_i - D\,E(\vec{F})\right)}{K_B T}\right) \qquad (4)$$

where $DE(F)$ is the electric field dependent barrier lowering:

$$\Delta E(\vec{F}) = \sqrt{\frac{q^3 F}{p\, e_s}} \qquad (5)$$

where q is the elementary charge and e_s is the permitivitty of silicon.

- Impact ionization by a free carrier; in this process the ionization rate depends directly on the carrier concentration ,n, and also depends on the ionization rate constant A_{ii} [1]

$$e_{ii} \propto n A_{ii}\left(E_i, \vec{F}, T\right) \qquad (6)$$

-Quantum-mechanical tunneling; the trapped carriers tunnel to the respective free band when the Coulombic potential barrier drops due to the electric field. This mechanism dominates at higher electric fields and is given by [21]

$$A_{TUN}(\vec{F}) = \left[\frac{U(\vec{F})}{3\hbar}\right]\sqrt{\frac{U(\vec{F})}{E_i}}\exp\left[-\left(\frac{E_i}{U(\vec{F})}\right)^{\frac{3}{2}}\right] \qquad (7)$$

where $U(\vec{F})$ is a characteristic energy that depends on the density-of-states effective mass for electrons, m^*_{de} :

$$U(\vec{F}) = \left(\frac{3q\hbar F}{4\sqrt{2m^*_{de}}}\right)^{\frac{2}{3}} \qquad (8)$$

-Phonon assisted tunneling; in this case the carrier is first excited thermally and then tunnels to the conduction band [22].

The regions of dominance of the ionization mechanisms in the plane $\vec{F} - T$ are shown in Fig. 4 [1]. The location of the domains depends highly on material conditions, such as the initial carrier concentration; hence, the figure is purely indicative.

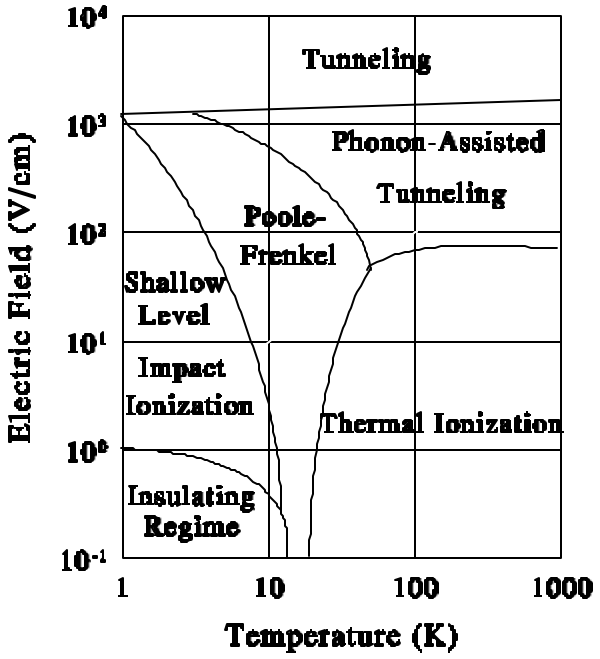

Figure 4. Dominance region of several mechanisms responsible for the ionization of impurities at low temperatures [1].

3. Time constants at low temperatures

In this section, the thermal and several electrical time constants are calculated as a function of temperature and compared to each other. In spite of its great importance under deep cryogenic conditions and low electric fields, the relaxation time for shallow level impact ionization is not considered. This is because the emission rate depends strongly on the nonequilibrium carrier concentration, which is not possible to determine in closed form [1].

The time constants considered here belong to the different mechanisms that may lead to the relaxation of the depletion region and the calculations are for a nondegenerate, uncompensated phosphorus-doped piece of silicon.

The Dielectric relaxation time is the time constant involved not with the impurity ionization process but with the redistribution of the majority carriers after the application of an external field. This relaxation time is simply expressed by:

$$t_{DIELECTRIC} = \frac{e_{Si}}{q m n} \qquad (9)$$

where e_{Si} is the silicon permittivity, q the elemental charge, m the electron mobility, and n the thermal equilibrium free carrier concentration. To know $n(T)$, one has to numerically solve the transcendental equation for the Fermi level referred to the conduction band, E_C-E_F, which results from the neutrality condition:

$$n(T) = N_D^+(T) + p(T) \qquad (10)$$

where $n(T)$ and $p(T)$ are, respectively, the thermal equilibrium electron and hole concentrations, and $N_D^+(T)$ is the concentration of ionized impurities. For the calculation of $n(T)$ and $p(T)$, Boltzmann statistics can be used; this is because the silicon is nondegenerate and E_F will be several K_BT below E_C for the temperatures considered here. Fermi-Dirac statistics are used to calculate $N_D^+(T)$, and (10) can be written as [25]:

$$N_C \exp\left(-\frac{E_C - E_F}{K_B T}\right) = N_D\left[1 - \frac{1}{1 + \frac{1}{2}\exp\left(\frac{(E_C - E_F) - E_i}{K_B T}\right)}\right] + N_V \exp\left(\frac{(E_C - E_F) - E_g}{K_B T}\right) \qquad (11)$$

where $N_C(T)$ and $N_V(T)$ are the effective density of states in the conduction and valence bands, respectively; N_D is the total concentration of impurities, Eg is the bandgap and E_i=E_C-E_D. In (10), all the temperature dependencies have not been included for simplicity. Once that E_C-E_F is numerically determined, $n(T)$ can be calculated by using the left-hand term of (11). Due to the lack of a more elaborated treatment for low temperatures [26], the three carrier scattering mechanisms considered here will be combined using Mathiessen's rule. This is a rough approximation because those mechanisms are not fully independent from each other. Hence, the total electron mobility is given by

$$\mu = \left(\mu_L^{-1} + \mu_I^{-1} + \mu_N^{-1}\right)^{-1} \qquad (12)$$

For the phonon scattering mechanism, the model of Sah et al. [27], which is valid for the 4.2 K<T<600 K temperature range, is taken for the lattice mobility:

$$\mu_L(T) = \frac{1}{\left[4195\left(T/300\right)^{-1.5}\right]^{-1} + \left[2153\left(T/300\right)^{-3.13}\right]^{-1}} \qquad (13)$$

The scattering by ionized impurities is modeled with a simplified form of the expression derived by Conwell and Weiskopf [28]:

$$\mu_I(T) = \frac{64 e_{Si}^2 (2K_B T)^{1.5}}{q^3 N_D^+(T)} \sqrt{\frac{p}{m_c^*}} \qquad (14)$$

where m_c^* is the conductivity effective mass for electrons, which also depends on temperature through the dependence on temperature of the transversal effective mass, m_t^*, and the longitudinal effective mass, m_l^*, [25]:

$$m_c^* = \left[\frac{1}{3}\left(\frac{2}{m_t^*} + \frac{1}{m_l^*} \right) \right]^{-1} \qquad (15)$$

Finally, the scattering by neutral impurities is considered. For uncompensated materials, this mechanism might be dominant at temperatures below 50 K [26]:

$$m_N(T) = \frac{q}{20 a_B \hbar \left(N_D - N_D^+(T) \right)} \left(\frac{m_c^*}{m_0} \right) \left(\frac{\varepsilon_0}{\varepsilon_{Si}} \right) \qquad (16)$$

where a_B is Bohr's radius, ε_0 is the permittivity of the free space and m_0 is the free electron mass.

Electron concentration and electron mobility are plotted in Fig. 5 for several values of the total doping concentration. These curves were found by solving the system formed by (10)-(16).

To obtain the relaxation time characteristic of the Poole-Frenkel mechanism, one must take the kinetic equation describing the ionization-trapping rate by impurities in the silicon [24]:

$$\frac{dN_D^+}{dt} = A_{PF}\left(N_D - N_D^+ \right) - nB_T N_D^+ \qquad (17)$$

where A_{PF} and B_T are the emission rate and the thermal recombination rate, respectively.

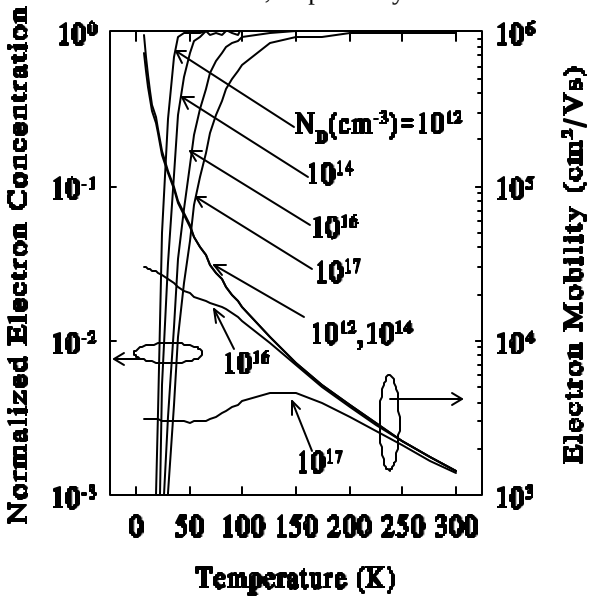

Figure 5. Calculated electron concentration and electron mobility as a function of temperature for several values of the doping concentration. These results are valid for a phosphorus doped uncompensated sample of silicon.

By assuming no spatial variation of the ionized doping concentration, (17) can easily be solved for $N_D^+(T)$, obtaining an exponential solution with a time constant given by

$$\tau_{PF}(T,\vec{F}) = \frac{1}{A_{PF} + nB_T} \qquad (18)$$

The emission rate is given by and (4) and (5). The thermal recombination rate, on the other hand, can be assumed not to be affected by the electric field [24]. In any case, in the regions where the electric field is important, the whole term nB_T is negligible, since according to Boltzmann's statistics n is very low.

A detailed balance applied to (17) under zero-field conditions then leads to

$$B_T(T) = \frac{A_{PF}(\vec{F}=0)}{n(T)} \left(\frac{N_D}{N_D^+(T)} - 1 \right) \qquad (19)$$

where $A_{PF}(\vec{F}=0)$ is the zero-field Poole-Frenkel emission rate, i.e., the pure thermal emission rate. *n(T)* is simply the thermal equilibrium electron concentration calculated by using (10) and (11).

The treatment for the relaxation time characteristic of quantum-mechanical tunneling mechanism is similar to that for the Poole-Frenkel. The only difference is that now the emission rate will be given by (7) and (8):

$$\tau_{TUN}(T,\vec{F}) = \frac{1}{A_{TUN} + nB_T} \qquad (20)$$

The time constants expressed by (18) and (20) are plotted in Fig. 6 for two extreme doping concentrations and several values of the electric field. The dielectric and thermal time constants are also included for comparison. The former is the one calculated using (9) and the results shown in Fig. 5 for electron concentration and mobility. The latter was taken from Fig. 3.

Many interesting facts can be observed in Fig. 6.a) for temperatures around 300 K. The limiting process for the relaxation of the depletion region is simply the dielectric one. It is the longest of the electrical time constants. The tunneling process can be much slower for electric fields lower than 10^5 V/cm; however, it is unimportant as the relaxation by pure thermal ionization (zero-field Poole-Frenkel) is much faster. So that, the latter is the dominant impurity ionization process and is much slower than the dielectric one. A slight difference can be observed when the impurity concentration is incremented by 5 orders of magnitude, as shown in Fig. 6.b).

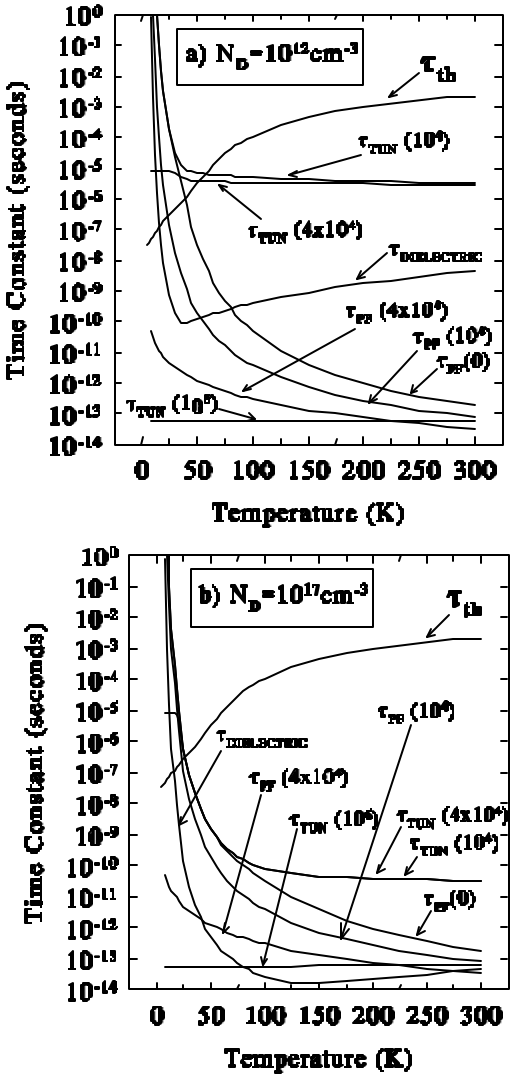

Figure 6. The thermal and several electrical time constants as a function of temperature, for a) $N_D=10^{12}$ cm^{-3}, and b) $N_D=10^{17}$ cm^{-3}. The value of the electric field is indicated in parentheses for the Poole-Frenkel and Tunneling mechanisms.

In this case, the dielectric time seems to be shorter than the pure thermal ionization time constant. It then suggests that the limiting process is the ionization of impurities. Nevertheless, these times are of the same order of magnitude (10^{-13} s), and are so short that the distinction between them becomes meaningless. For both extreme doping concentrations, the thermal time constant is from 6 to 10 orders of magnitude longer than any other; hence, the RT heat transfer is much slower than the relaxation of the depletion region. As the temperature decreases, all the electrical time constants increase, while the thermal one decreases monotonically. No qualitative change is observed from room temperature to around 100 K; the heat transfer is still the slowest process. However, for temperatures below 50 K and low electric fields, no matter what the doping concentration is and which process limits the formation of the depletion region, the thermal time constant is of the same order of magnitude that the electrical time constants.

According to Fig. 6, the thermal time constant may even be the shortest under deep cryogenic conditions, below 30 K. As was already established, this picture changes when high electric fields are applied to the silicon sample. In such cases, the field-activated time constants become several orders of magnitude shorter than any other making the relaxation of the depletion region much faster than the transfer of heat.

4. Conclusions

Some published experimental results on transient SH of Si devices at very low temperature were discussed in this work; these showed a very disperse set of data, making it too difficult for any quantitative comparison. The source of such differences may be partially attributed to particularities inherent to every experiment. The erroneous assumptions upon which the TDC experimental procedure was based, gave place to many anomalies for the temperature rises and time constants reported.

The thermal time constant for a typical silicon die was calculated for the temperature range from 300 K to 4.2 K. This was compared to several electrical time constants that characterize the relaxation of the depletion region. This estimation leads to the conclusion that any transient phenomenon under deep cryogenic conditions must be due to the combined effect of both electrical and heat transfer phenomena. This is because their time constants are of the same order of magnitude for relatively low electric fields.

Acknowledgements

This work was supported by CONACyT under grant I32891-A.

References

[1] B. Dierickx, *Transient Phenomena and Noise in Silicon MOSFETs at Cryogenic Temperatures*, Ph.D. dissertation, Katholieke Universiteit Leuven, Belgium (1990).

[2] J. Wolf, U. Grözinger and D. Lemke, in Low Temperature Electronics and High Temperature Superconductivity/1995, C. Claeys, S.I. Raider, R.K. Kirschman and W.D. Brown, Editors, PV 95-9, pp. 355-368, The Electrochemical Society Proceedings Series, Pennington, NJ (1995).

[3] E.A. Gutiérrez-D., *Electrical Performance of Submicron CMOS Technologies from 300 K to 4.2 K*, Ph.D. dissertation, Katholieke Universiteit Leuven, Belgium (1993)

[4] Y.S. Touloukian, R.W. Powell, C.Y. Ho, and P.G. Clemens, The TPRC Data Series, Vols. 1&2, (IFI/Plenum, New York, 1970).

[5] J. Callaway, Phys. Rev. **113**, 1046 (1959).

[6] J. Callaway, Phys. Rev. **122**, 787 (1961).

[7] C.J. Glassbrenner and G.A. Slack, Phys. Rev. A., **134,** A1058 (1964).

[8] J. P. McKelvey, Solid State and Semiconductor Physics, (Harper and Row Pub., 1966).

[9] F.J. De la Hidalga-W., *Low Temperature Modeling and Simulation of Semiconductor Devices*, Ph.D. dissertation, INAOE, Puebla, Mexico, (1998).

[10] E.A. Gutiérrez-D., D.L. Deferm and G. Declerck, IEEE Trans. Electron Dev. Letters, **14,** 152 (1993).

[11] S.S. Sesnic and G.R. Craig, IEEE Trans. Electron Dev., **19,** 933 (1972).

[12] D.P. Foty and S.L. Titcomb, IEEE Trans. Electron Dev., **34,** 107 (1987).

[13] D.P. Foty, IEEE Trans. Electron Dev., **36,** 1542 (1989).

[14] E.A. Gutiérrez-D, D.L. Deferm and G. Declerck, Solid-State Electronics, **36,** 41 (1993).

[15] F.J. De la Hidalga-W. and E.A. Gutiérrez-D., in Low Temperature Electronics and High Temperature Superconductivity/1997, C. Claeys, S.I. Raider, M.J. Deen, W.D. Brown and R.K. Kirschman, Editors, PV 97-2, pp. 387-394, The Electrochemical Society Proceedings Series, Pennington, NJ (1997).

[16] F.J. De la Hidalga-W, M.J. Deen, E.A. Gutiérrez-D and F. Balestra, Electronics Letters, **33,** 1456 (1997).

[17] R. Vogelsong and C. Brzezinski, *Extending SPICE for Electrothermal Simulation*, in Proc. CICC, San Diego, CA, 21.4.1, May (1989).

[18] A.G. Milnes, Deep Impurities in Semiconductors, (Wiley-Interscience, New York, 1973) p. 91.

[19] N.S. Saks and A. Nordbryhn, J. Appl. Phys., **50**, 6962 (1979).

[20] D.P. Foty, Cryogenics, **30**, 1056 (1990).

[21] Hui-Quan Nie, D.D. Coon, Solid-State Electronics, **27,** 53 (1984).

[22] J.R. Banavar, D.D. Coon, G.E. Derbits, Phys. Rev. Lett, **41,** 576 (1978).

[23] E. Rosencher, V. Mosser and G. Vincent, Solid State Communications, **45,** 629 (1983).

[24] E. Rosencher, V. Mosser and G. Vincent, Phys. Rev. B, **29,** 1135 (1984).

[25] S.M. Sze, Physics of Semiconductor Devices, 2nd Ed., (Wiley & Sons, Singapore, 1981).

[26] S. Selberherr, Analysis and Simulation of Semiconductor Devices, (Springer, New York, 1984).

[27] C.T. Sah, P.C.H. Chan, C.K. Wang, R.L.Y. Sah, K.A. Yamakawa and R. Lutwack, IEEE Trans. On Electron Devices, **28,** 304 (1981).

[28] E. Conwell and V.F. Weisskopf, Phys. Rev. **77,** 388 (1950).